J|A|C|S COMMUNICATIONS

Published on Web 08/17/2009

Shape and Size Effects of ZnO Nanocrystals on Photocatalytic Activity

Anna Mclaren, Teresa Valdes-Solis, Guoqiang Li, and Shik Chi Tsang*

Wolfson Catalysis Centre, Inorganic Chemistry Laboratory, University of Oxford, Oxford OX1 3QR, U.K.

Received June 30, 2009; E-mail: Edman.tsang@chem.ox.ac.uk

Zinc oxide is a direct wide-band-gap semiconductor with a band gap of 3.37 eV.[1] This fact, coupled with its large exciton binding energy of 60 meV[1] (at room temperature), means that ZnO is suitable for use in a wide range of optical and electronic applications. It is also notable that ZnO is biocompatible and exhibits high mechanical, thermal, and chemical stability. Thus, a wide range of applications, including its use in UV lasers,[2] field-effect transistors,[3] photodetectors,[4] gas sensors,[5] solar cells,[6] piezoelectric generators,[7] and photocatalysis,[8,9] is envisaged. The potential use in photocatalysis (e.g., photolysis of water to generate hydrogen, photodecomposition of organics) has particularly aroused great interest, as there have been several examples of ZnO displaying more impressive photocatalytic activity than widely studied titanium dioxide.[8] Also, the quantum efficiency of ZnO has been shown to be higher.[9] The ability to control particle morphology is an important objective in nanocrystal synthesis, as size and shape can significantly influence various properties.[10,11] A pronounced effect of ZnO morphology on thin films for optical and electronic applications has been reported, but little work has been done to investigate the morphological effect on photocatalytic activity in solvent. Difficulties are anticipated, as traditional research using single-crystal surfaces in a UHV system is not applicable. Here we report a simple solution method for tailoring the degree of extended growth of ZnO nanoparticles (NPs) along the <0001> axis, giving regular hexagonal platelike nanocrystals at one extreme and various lengths of hexagonal rods at the other. The hexagonal platelike particles were found to display *>5 times higher* activity in the photocatalytic decomposition of methylene blue than the rod-shaped particles. This clearly suggests that the terminal polar (001) and (00$\bar{1}$) faces are more active surfaces for photocatalysis than the nonpolar surfaces perpendicular to them (i.e., 100, 101).

The synthesis was based on the modified method by Andelman et al.[12] with further new study of the variation of the oleic acid (OA)/zinc acetate (ZnAc) ratio and the adopted surface pretreatment according to Sun et al.[13] [see the Supporting Information (SI)]. X-ray diffraction (XRD) data confirmed that all of the samples produced were crystalline and had the hexagonal wurtzite structure of bulk ZnO with lattice parameters matching those in the literature. It was found that an increase in the solvent/OA molar ratio (decreasing OA concentration) led to an increase in average NP size (Figure 1a). This is the anticipated effect, as the role of OA in the reaction system is not only to stabilize the NPs against agglomeration but also to hinder their growth. When bound to NP surfaces, OA molecules can provide steric hindrance to molecular addition to the NPs. The OA concentration also apparently affects the shape of the NPs formed. The three largest characteristic (100), (002), and (101) peaks for various samples are shown in Figure 1b. The relative intensities of the peaks for samples with OA/Zn^{2+} ratios of 0.4 and 4.0 closely resemble that of bulk ZnO. However, for intermediate ratios, the (002) peak greatly increases in relative intensity as the ratio increases from 1, reaching a maximum at a ratio of 2, and then decreases for ratios greater than 2. This enhancement in the (002) peak has been observed previously and attributed to the formation of nanorods oriented along the *c* axis at these intermediate ratios (the increased relative intensity reflects the larger number of planes along the long axis of the rod[14,15]).

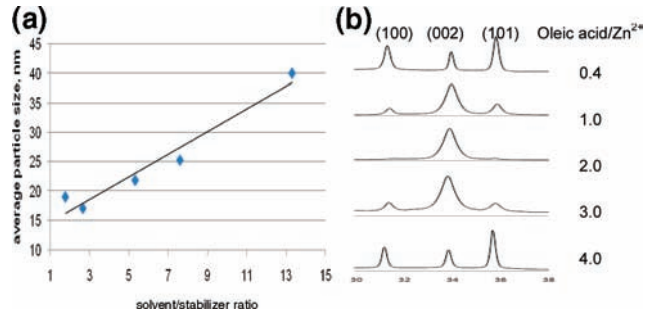

Figure 1. (a) Graph showing the change in average particle size with changing trioctylamine/OA ratio (using 33.93 mmol of trioctylamine, 6.38 mmol of ZnAc, and varying OA concentration). (b) Relative intensities of the three major XRD peaks [*x*-axis unit is 2θ (deg)] for samples with different OA/Zn^{2+} ratios [same compositions as in (a)].

The TEM images in Figure 2b indeed show the formation of rod structures. The average rod length increased from 210 to 230 nm while the diameter stayed relatively constant (24−29 nm) as the OA/Zn^{2+} ratio was changed from 1 to 2 (see the SI). The change in relative peak intensities was greatest for NPs synthesized with a OA/Zn^{2+} ratio of 2, which also exhibited the highest aspect ratio (∼9). It is interesting that the growth along [0001] was dramatically suppressed for OA/Zn^{2+} ≥ 4, giving a hexagonal platelike structure with a similar diameter (but larger than those reported by Yin et al.[15]).

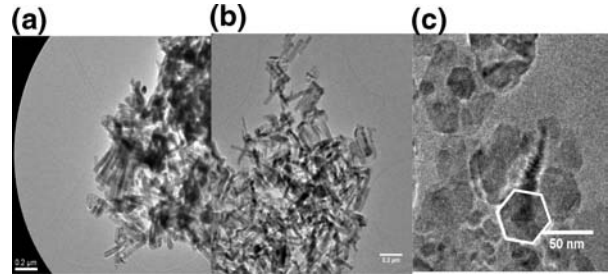

Figure 2. TEM images of samples synthesized with OA/Zn^{2+} ratios of (a) 1, (b) 2, and (c) 4.

The growth of the long ZnO rods from hexagonal planar ZnO seeds during the solvothermal process on zinc foil has been discussed.[16] The hexagonal wurtzite ZnO with a polar structure can be described as hexagonal-close-packed O and Zn atoms in point group 6*mm* and space group $P6_3mc$ with Zn atoms in tetrahedral sites. Thus, the crystal habits of wurtzite ZnO exhibit well-defined crystallographic faces, i.e., basal (001) parallel to (002) and nonpolar low-symmetry (100) faces (and C_{6v}-symmetric ones). In the case of wurtzite ZnO crystals, the Zn-terminated (001) planes are active in promoting one-dimensional growth. Thus, one face of the hexagonal sheet is Zn-rich and forms the (001) plane, whereas the opposite face is the (00$\bar{1}$) plane. For a crystal growing under kinetic control, the shape may be related to the growth rates of the two faces, with the fastest-growing planes disappearing to leave behind the slowest-growing planes as the crystal facets. The presence of the capping agent (stabilizer) that binds to a

10.1021/ja9052703 CCC: $40.75

face changes the free energy of that face and hence slows its growth. In this case, it is apparent that the combination of OA and trioctylamine capping agents in some ratios supports this preferential growth of the [0001] direction. Substituting the amine with decanol does not give the ZnO rod structure. We reported previously that a self-assembled lamella structure can be formed in organic solvent when OA and amine are coordinated with added cations. These cations and the polar end groups with hydrogen-bonding interactions from the capping agents take residence in the hydrophilic channels within the lamella structure.[17] Such layered supramolecular structures were clearly visible in the low-angle diffraction study (see the SI). The formation of ZnO nanorods with an increasing degree of anisotropy (increasing aspect ratio) that reaches a maximum at $OA/Zn^{2+} = 2$ is attributed to the two bidentate acid groups (H-bonded with amine) coordinated tetrahedrally with the zinc cation. During the thermal decomposition of ZnAc in the lamella template, the wurtzite ZnO product with the highest-energy (001) zinc face grows along the hydrophilic channel, so it is perhaps unsurprising that they were elongated in the [0001] direction while the capping agents would block the growth of (100), (101), and other faces perpendicular to the rod axis. At higher or lower ratios, the assembly is expected to be unstable and may switch from lamella (rod ZnO) to another morphology.

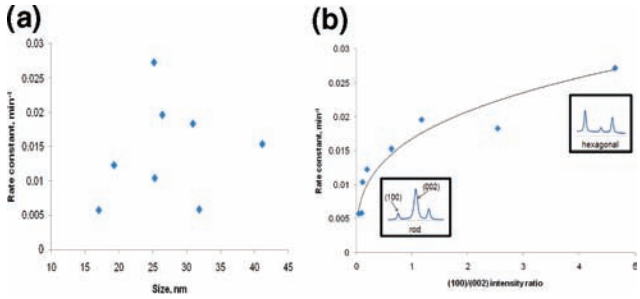

Figure 3. (a) Plot of photodecomposition rate constants of methylene blue vs average ZnO particle size. (b) Plot of the rate constants vs (100)/(002) intensity ratio.

Figure 3a shows a plot of photocatalytic activity in the decomposition of methylene blue in aqueous solution (see the SI for rate constant measurements) versus the average ZnO particle size. The data clearly indicate no apparent dependence of activity on particle size. Instead, the shape factor seems to be of overriding importance. It was noted earlier that the changing relative intensity of the (100) and (002) peaks in the XRD patterns of the materials corresponds to a change in particle shape. An XRD pattern collected for bulk, isotropic ZnO gave a value of 1.17 for the (100)/(002) intensity ratio, so deviations from this indicate a degree of particle anisotropy. An intense (002) peak [or a small (100)/(002) ratio] indicates the formation of rods oriented along the *c* axis. Conversely, a very large (100)/(002) ratio is indicative of shortening along the *c* axis. Figure 3b shows a plot of the rate constant versus this parameter (the same set of samples as for the size data was used). It can clearly be seen that rate constant increases with increasing (100)/(002) XRD peak intensity, corresponding to a >5-fold increase in the activity of the hexagonal platelike particles relative to the rod-shaped particles. The rod-shaped particles with the highest aspect ratio (rod length divided by diameter) show the poorest photocatalytic activity. Thus, there could still be a size effect in the observed fluctuation in photocatalytic activity among the samples with various particle sizes, but the dominant shape effect appears to mask the size effect. A significant difference between particles of differing morphologies is the proportion of different crystal facets present on the surface of the particles. The surface of a *c*-axis-aligned rod mostly consists of nonpolar faces parallel to the rod axis, whereas the dominant surfaces exposed on a hexagonal plate with the same diameter are the polar (001) Zn face and the $(00\bar{1})$ O face (enlarged for clarity), as illustrated in Figure 4.

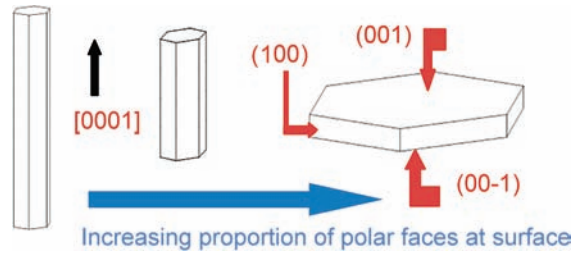

Figure 4. Diagram showing the dominant facets present on the surfaces of NPs with different shapes.

The data clearly implies that exposure of a greater proportion of polar faces leads to greater photocatalytic activity. The high activity of the (001) Zn face could be attributed to the (001) face of ZnO, the face with the intrinsically highest energy among all the faces. The OH^- ions could preferentially adsorb onto this face because of its positive charge.[18] This would lead to a greater rate of production of $OH^{\cdot}$ radicals, and hence degradation of the dye, during the photocatalysis. It is interesting to note that the recent results from Li et al.[19] may provide an alternative new insight. They have discovered a positive correlation between the proportion of polar faces exposed and the surface oxygen vacancy content of samples, as evidenced by photoluminescence spectroscopy. Oxygen vacancies in ZnO undoubtedly can act as potential wells to trap either one or two electrons, aiding electron−hole pair separation and hence increasing the photocatalytic activity. Further experiments are therefore needed in order to address the origin of the high photocatalytic activity of the polar faces reported in this note.

Supporting Information Available: Experimental procedures and materials characterization. This material is available free of charge via the Internet at http://pubs.acs.org.

References

(1) Wang, Z. L. *ACS Nano* **2008**, *2*, 1987.
(2) Huang, M. H.; Mao, S.; Feick, H.; Yan, H. Q.; Wu, Y. Y.; Kind, H.; Weber, E.; Russo, R.; Yang, P. D. *Science* **2001**, *292*, 1897.
(3) Goldberger, J.; Sirbuly, D. J.; Law, M.; Yang, P. *J. Phys. Chem. B* **2005**, *109*, 9.
(4) Kind, H.; Yan, H. Q.; Messer, B.; Law, M.; Yang, P. D. *Adv. Mater.* **2002**, *14*, 158.
(5) Wan, Q.; Li, Q. H.; Chen, Y. J.; Wang, T. H.; He, X. L.; Li, J. P.; Lin, C. L. *Appl. Phys. Lett.* **2004**, *84*, 3654.
(6) Keis, K.; Vayssieres, L.; Lindquist, S. E.; Hagfeldt, A. In *Nanostructured ZnO Electrodes for Photovoltaic Applications*, Proceedings of the Fourth International Conference on Nanostructured Materials (Nano98), Stockholm, Sweden, June 14−19, 1998; pp 487−490.
(7) Wang, Z. L.; Song, J. H. *Science* **2006**, *312*, 242.
(8) Lizama, C.; Freer, J.; Baeza, J.; Mansilla, H. D. *Ibero-American Workshop on Photocatalysis, Seville, Spain*; Elsevier Science BV: Seville, Spain, 2002; pp 235−246.
(9) Sakthivel, S.; Neppolian, B.; Shankar, M. V.; Arabindoo, B.; Palanichamy, M.; Murugesan, V. *Sol. Energy Mater. Sol. Cells* **2003**, *77*, 65.
(10) Ischenko, V.; Polarz, S.; Grote, D.; Stavarache, V.; Fink, K. *Adv. Funct. Mater.* **2005**, *15*, 1945.
(11) Gao, P. X.; Ding, Y.; Wang, I. L.*Nano Lett.* **2003**, *3*, 1315. Zhang, N.; Yi, R.; Shi, R. R.; Gao, G. H.; Chen, G.; Liu, X. H. *Mater. Lett.* **2009**, *63*, 496.
(12) Andelman, T.; Gong, Y. Y.; Polking, M.; Yin, M.; Kuskovsky, I.; Neumark, G.; O'Brien, S. *J. Phys. Chem. B* **2005**, *109*, 14314.
(13) Sun, S. H.; Zeng, H.; Robinson, D. B.; Raoux, S.; Rice, P. M.; Wang, S. X. *J. Am. Chem. Soc.* **2004**, *126*, 273.
(14) Zhu, Z. M.; Andelman, T.; Yin, M.; Chen, T. L.; Ehrlich, S. N.; O'Brien, S. P.; Osgood, R. M. *J. Mater. Res.* **2005**, *20*, 1033.
(15) Yin, M.; Gu, Y.; Kuskovsky, I. L.; Andelman, T.; Zhu, Z. M.; Neumark, G. F.; O'Brien, S. *J. Am. Chem. Soc.* **2004**, *126*, 6206.
(16) Yang, J. H.; Zheng, J. H.; Zhai, H. J.; Yang, L. L.; Liu, L.; Gao, M. *Cryst. Res. Technol.* **2009**, *44*, 619.
(17) Huang, Y. Q.; Lin, Y.; Zeng, G.; Liang, Z. X.; Liu, X. L.; Hong, X. L.; Zhang, G. Y.; Tsang, S. C. *J. Mater. Chem.* **2008**, *18*, 5445.
(18) Dodd, A.; McKinley, A.; Tsuzuki, T.; Saunders, M. *Mater. Chem. Phys.* **2009**, *114*, 382.
(19) Li, G. R.; Hu, T.; Pan, G. L.; Yan, T. Y.; Gao, X. P.; Zhu, H. Y. *J. Phys. Chem. C* **2008**, *112*, 11859.

JA9052703